Electronic Supplementary Material (ESI) for RSC Advances

Remarkable Role of Positional Isomers in the Design of Sensors for the Ratiometric Detection of Copper and Mercury Ions in Water

Namita Kumari,[a] Nilanjan Dey[a] and Santanu Bhattacharya*[, a, b]

[a]Department of Organic Chemistry, Indian Institute of Science, Bangalore 560 012, India and [b]Chemical Biology Unit, JNCASR, Bangalore 560 064, India.

Contents

Compound **4**. White solid; (Yield: 39 mg, 74 %), ^{1}H NMR (400 MHz, $CDCl_3$) δ (ppm) 1.31 (t, *J* = 8 Hz, 6H), 1.86 (s, 6H), 3.28 (q, *J* = 4 Hz, 4H), 3.47 (s, 2H), 6.33 (s, 2H), 6.39 (s, 2H), 7.06 (t, *J* = 8 Hz, 1H), 7.24 (d, J = 2.8 Hz, 4H), 7.47 (t, *J* = 4 Hz, 2H), 7.50-7.53 (m, 4H), 8.01 (t, *J* = 4 Hz, 6H), 8.44 (s, 1H); ^{13}C NMR (100 MHz, $CDCl_3$) δ (ppm): 14.6, 16.6, 38.3, 65.7, 96.6, 106.1, 117.9, 123.3, 123.6, 127.4, 127.6, 128.6, 129.5, 133.4, 135.0, 146.3, 147.5, 151.2, 152.2, 165.1; HRMS *m/z* calcd for $C_{33}H_{32}N_4O_2$ $(M+Na)^+$ 539.2423, found 539.2423.

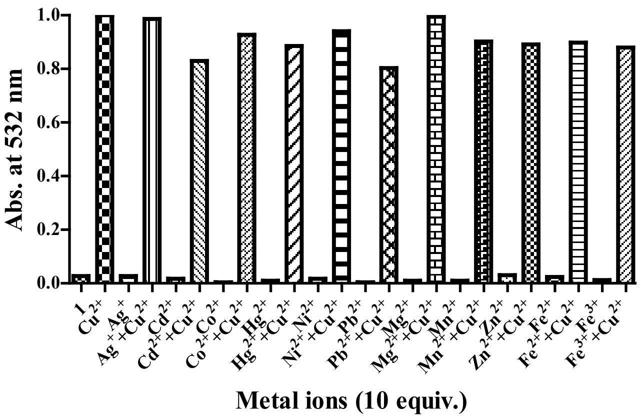

Fig. S1 Plot of normalized absorbance (at 532 nm) of **1** with added Cu^{2+} (2 equiv.) in presence of excess of other metal ions (10 equiv.) in water.

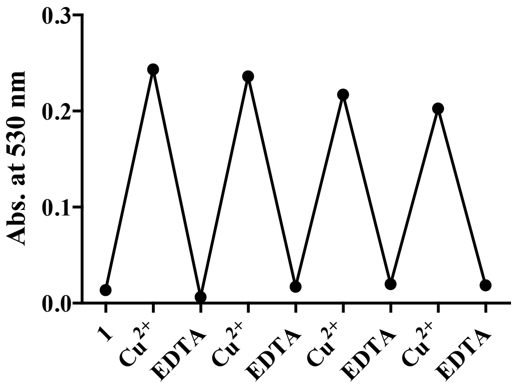

Fig. S2 Recovery of the molecular absorbance at 530 nm after addition of EDTA (5 equiv.) after each addition of 5 equiv. of Cu^{2+} to the sensor **1** (10 μM)

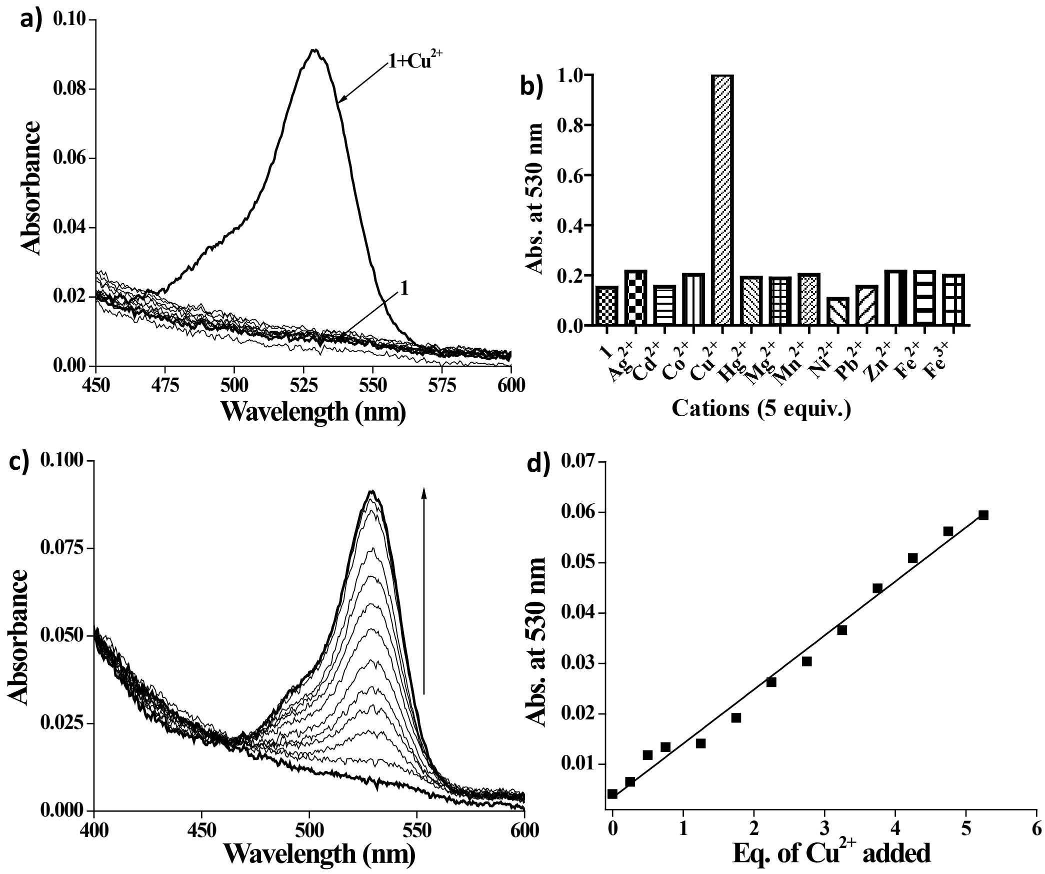

Fig. S3 (a) Absorption spectral changes of **1** (10 μM) at pH 7.4 (HEPES buffer, 0.05 M) upon addition of 5 equiv. of different salts of Ag^{+}, Cd^{2+}, Co^{2+}, Cu^{2+}, Fe^{2+}, Fe^{3+}, Hg^{2+}, Mg^{2+}, Mn^{2+}, Ni^{2+}, Pb^{2+} and Zn^{2+}. (b) Normalized absorbance of **1** (10 μM) at 530 nm after the addition of various cations (5 equiv.). (c) UV-Vis titration of **1** (10 μM) at pH 7.4 (HEPES buffer, 0.05M) with Cu^{2+} (0 to 55 μM). (d) Plot of absorbance at 530 nm against the added equivalent of Cu^{2+}.

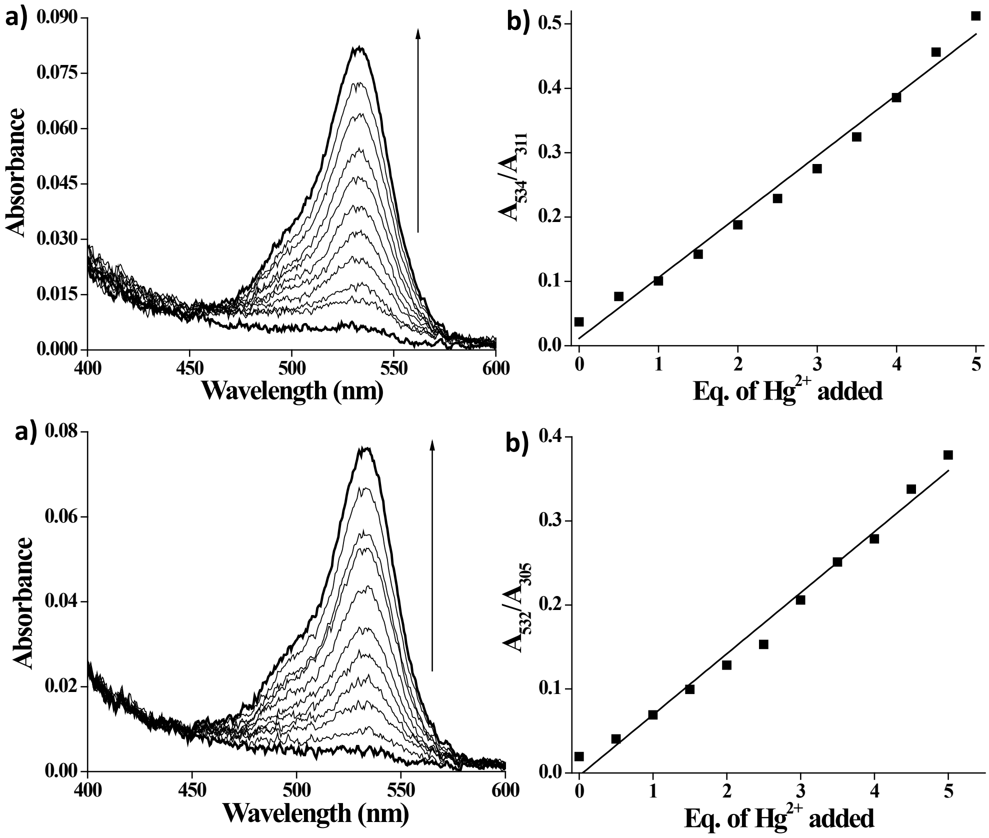

Fig. S4 Upper panel sensor **2** and lower panel sensor **3**; (a) UV-Vis titration of sensor **2** or **3** (10 µM) in water with Hg^{2+} (0 to 50 µM); (b) Ratiometric plot with equiv. of Hg^{2+} at the absorbance ratio of A_{534}/A_{311} nm for **2** and A_{532}/A_{305} nm for **3**.

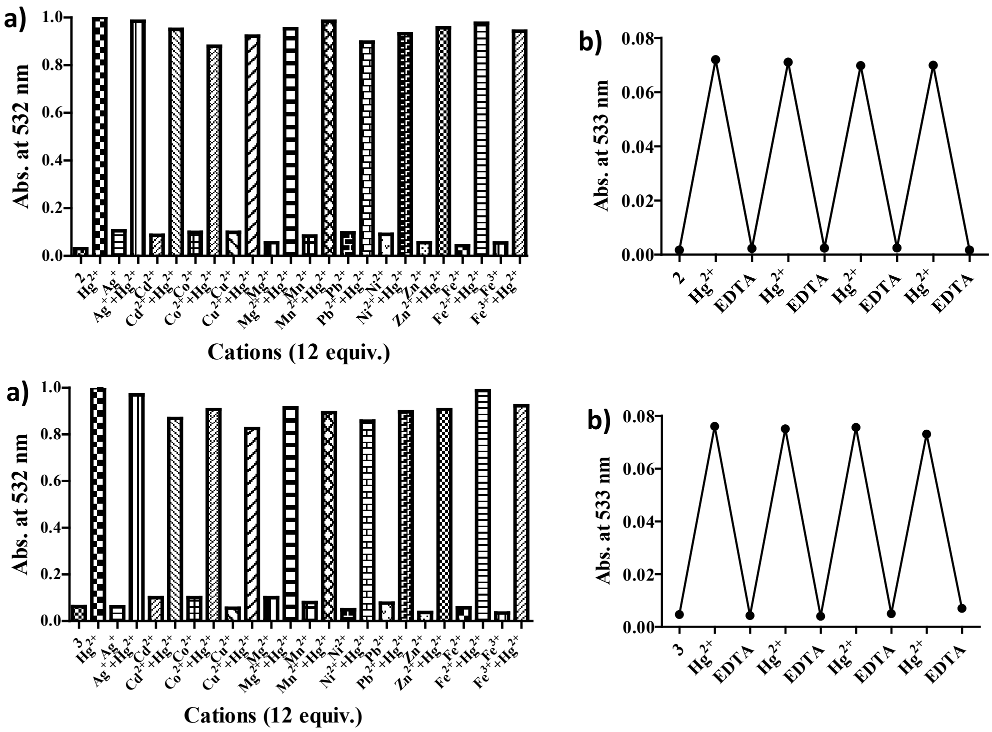

Fig. S5 Upper panel sensor **2** and lower panel sensor **3**; (a) Plot of normalized absorbance (at 532 nm) of the sensors **2** or **3** with Hg^{2+} (4 equiv.) in presence of an excess of other metal ions (12 equiv.). (b) Recovery of the molecular absorbance at 533 nm after addition of EDTA (10 equiv.) after each addition of 5 equiv. of Hg^{2+} to the sensor **2** or **3** (10 μM).

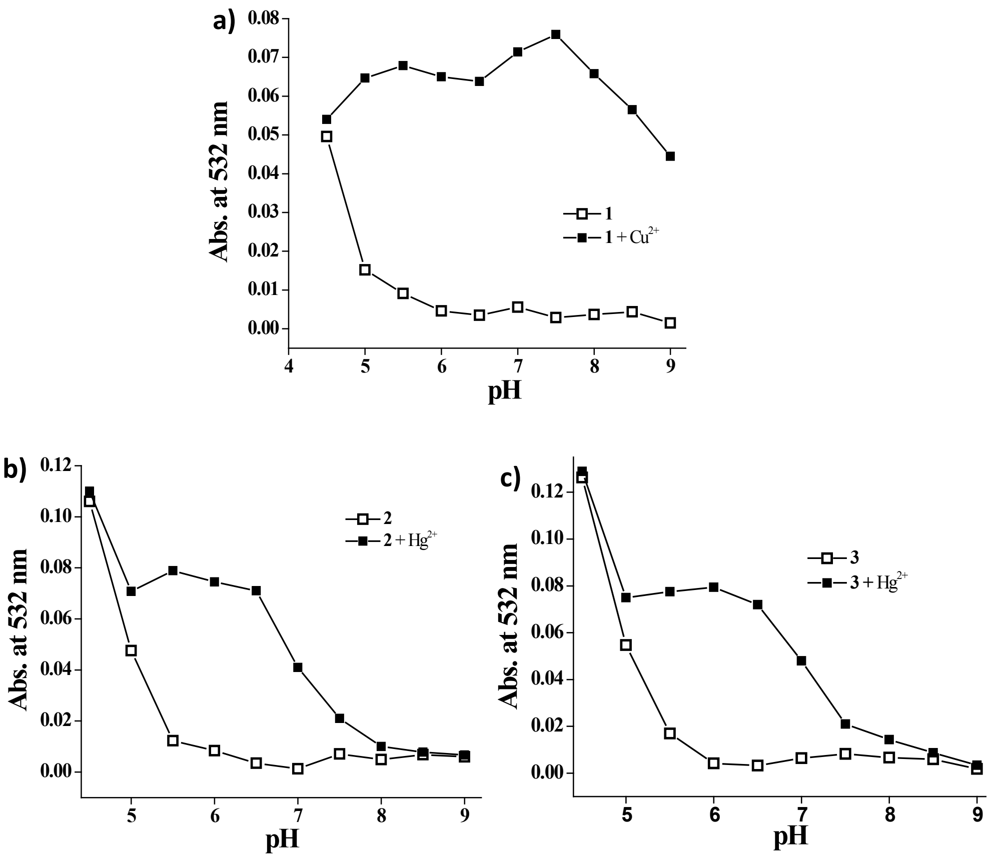

Fig. S6 (a) Plot of absorbance at 532 nm of **1** (10 µM) and after the addition of 5 equiv. of Cu^{2+} ion at different pH**.** (b) Plot of the absorbance at 532 nm of **2** (10 µM) and after the addition of 5 equiv. of Hg^{2+} ion at different pH**.** (c) Plot of the absorbance at 532 nm of **3** (10 µM) and after the addition of 5 equiv. of Hg^{2+} ion at different pH**.**

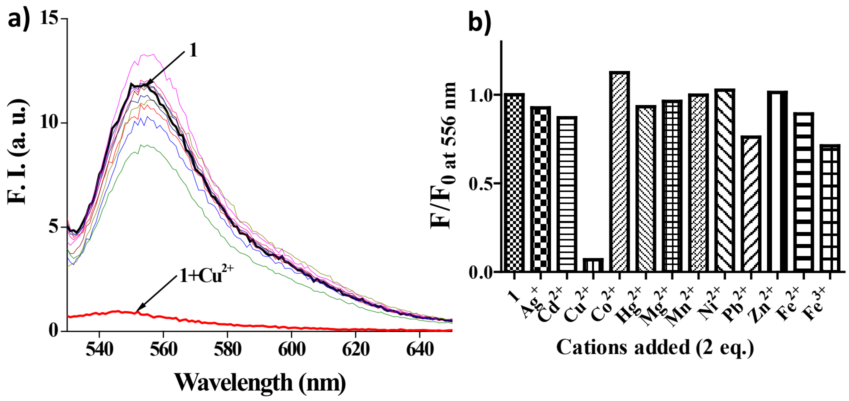

Fig. S7 (a) Fluorescence emission spectra of **1** (5 µM) in water (λ_{ex} = 520 nm) in the presence of various cations (2 equiv.). (b) Normalized spectra of the fluorescence intensity at 556 nm after the addition of each cation.

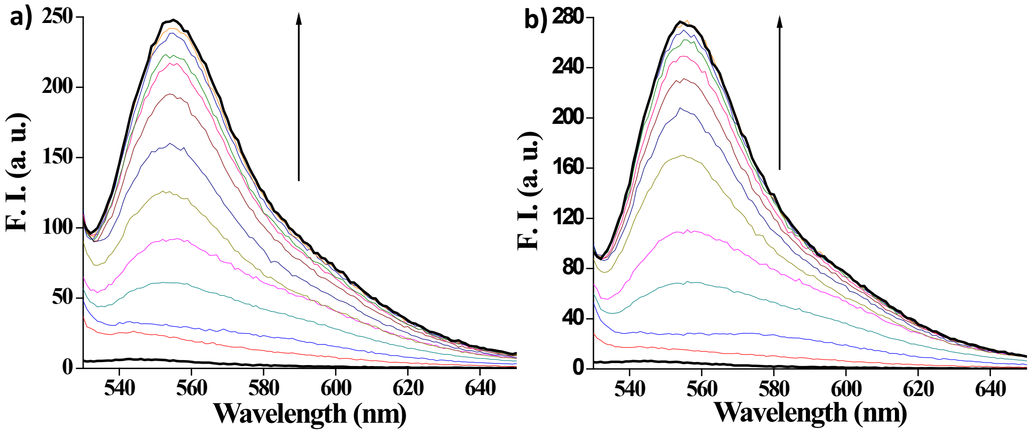

Fig. S8 Fluorescence titration of sensor (a) **2** and (b) **3** (5 μM) in water with Hg^{2+} (0 – 5 equiv.) (λ_{ex} = 520 nm).

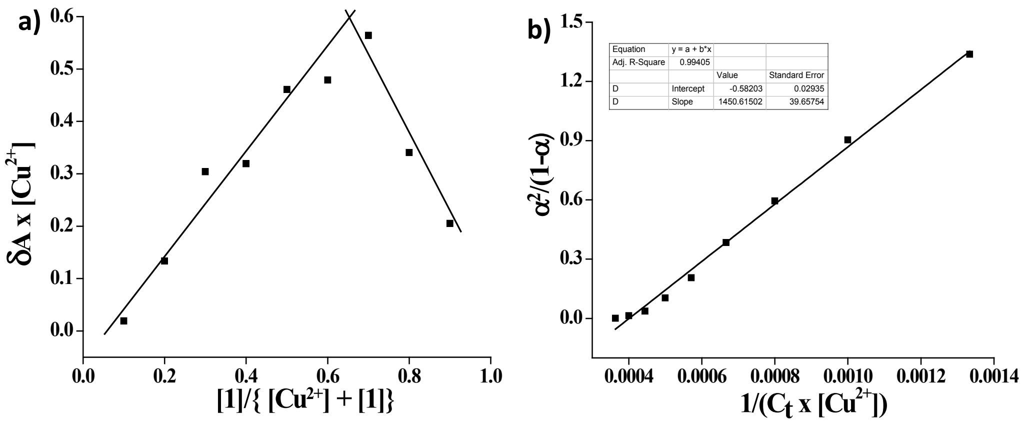

Fig. S9 (a) Job plot analyses of **1** demonstrating 2:1 binding with the Cu^{2+} ion. [δA = change in the absorbance; The total concentration [**1**] + [Cu^{2+}] = 1.0× 10^{-4} M.] (b) Binding constant was calculated using Benesi-Hildebrand equation for the 2:1 stoichiometry.

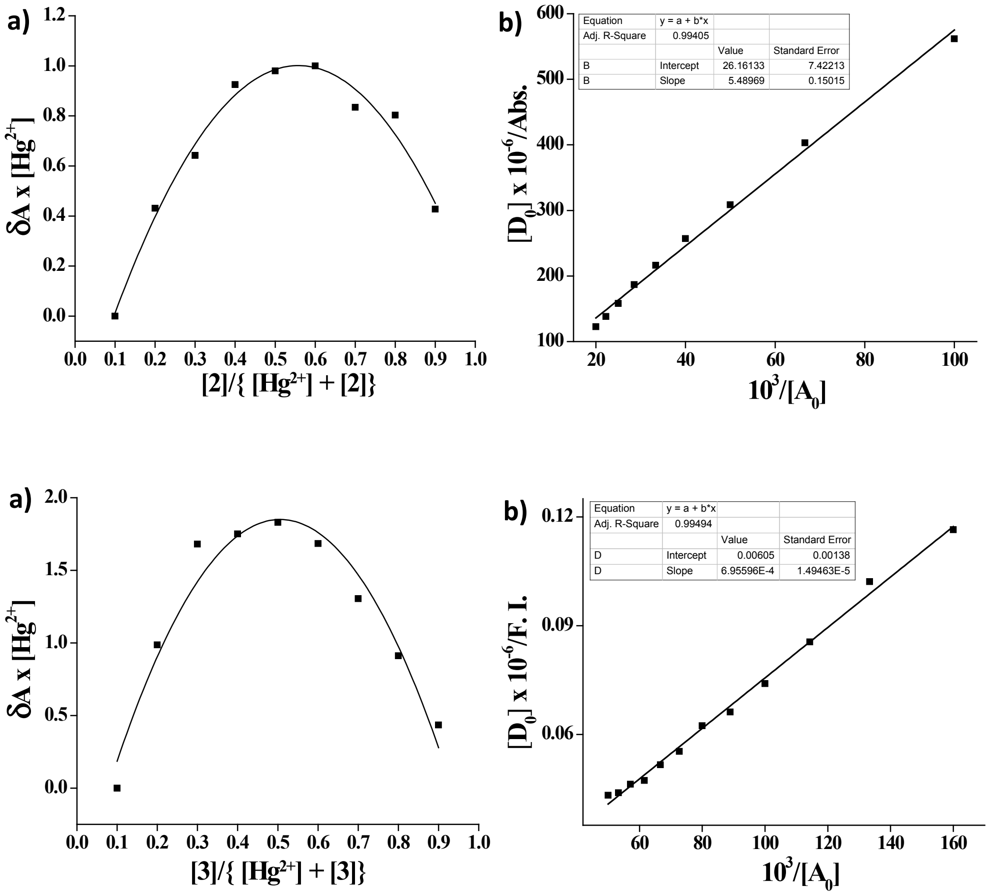

Fig. **S10** Upper panel sensor **2** and lower panel sensor **3**; (a) Job plot analyses of sensor **2** or **3** demonstrating 1:1 binding with Hg^{2+} ion. (δA = change in the absorbance; The total concentration [sensor] + [Hg^{2+}] = 1.0×10^{-4} M) (b) Binding constant calculation employed Benesi-Hildebrand equation with 1:1 stoichiometry.

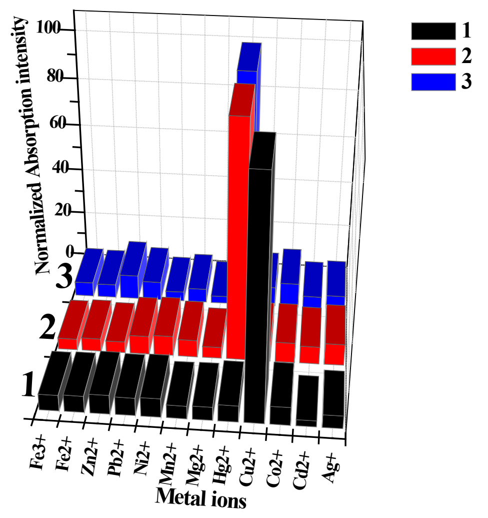

Fig. S11 The selectivity coefficients for the heavy metal ions in terms of the relative enhancement in absorbance of probe.

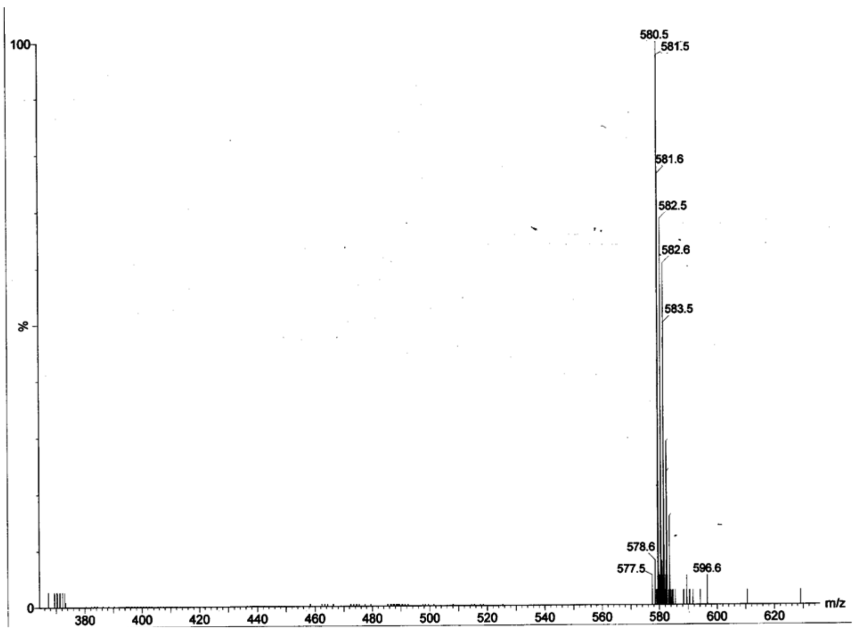

Fig. S12 Mass spectrum of **1**-Cu^{2+} $[L_2.Cu.2MeOH]^{2+}$.

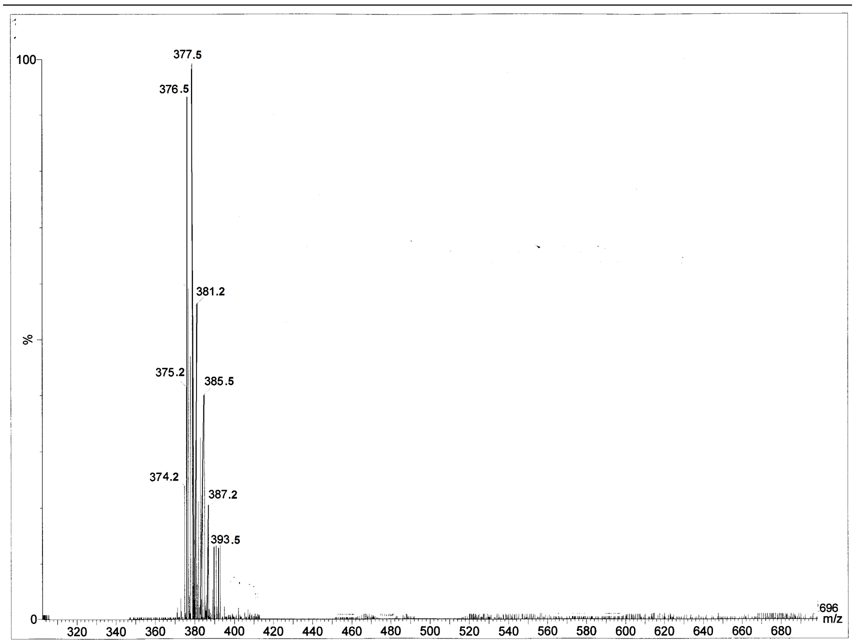

Fig. **S13** Mass spectrum of **2**-Hg^{2+} $[L.Hg.2H_2O]^{2+}$.

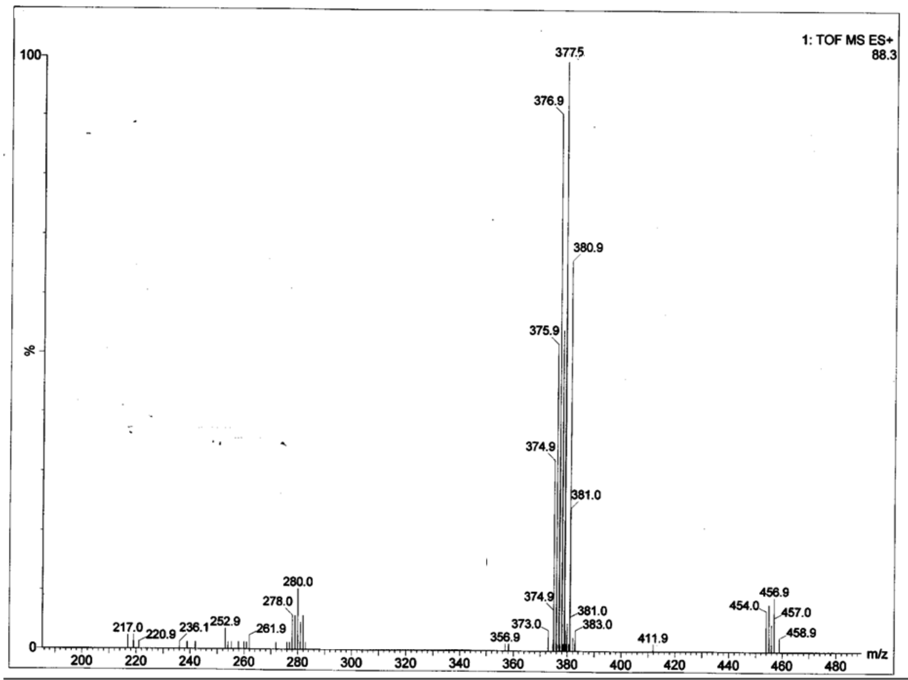

Fig. **S14** Mass spectrum of **3**-Hg^{2+} $[L.Hg.2H_2O]^{2+}$.

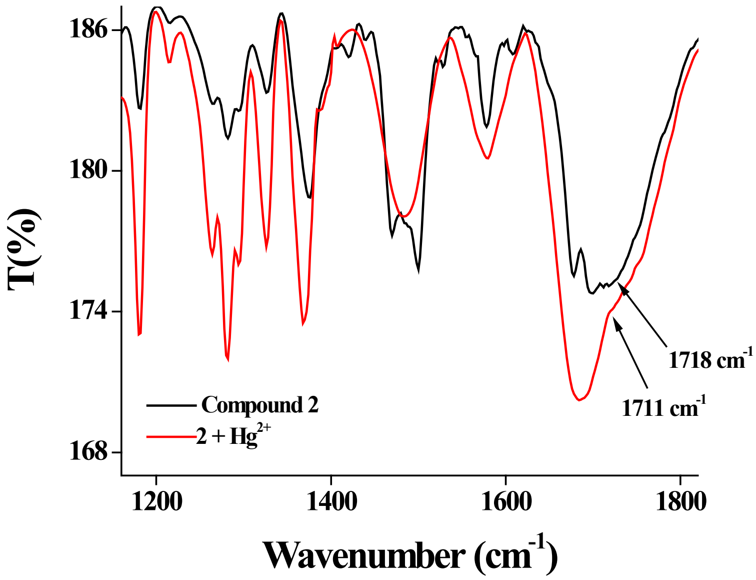

Fig. **S15** FT-IR spectrum of **2** and **2**-Hg^{2+}.

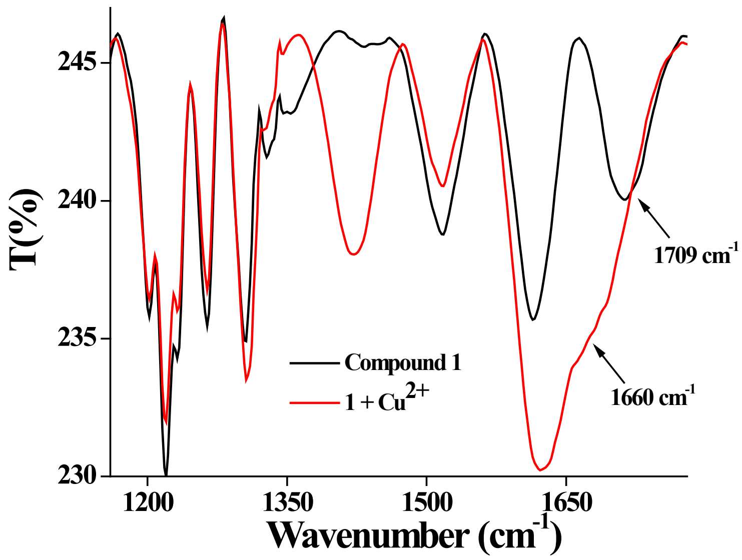

Fig. **S16** FT-IR spectrum of **1** and **1**-Cu^{2+}.

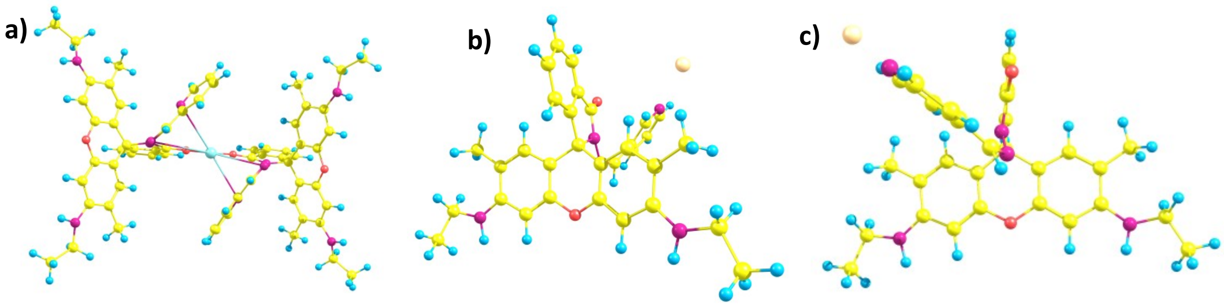

Fig. S17 DFT optimized structures of **1**-Cu^{2+}, **2**-Hg^{2+} and **3**-Hg^{2+} using B3LYP functional and LANL2DZ basis set.

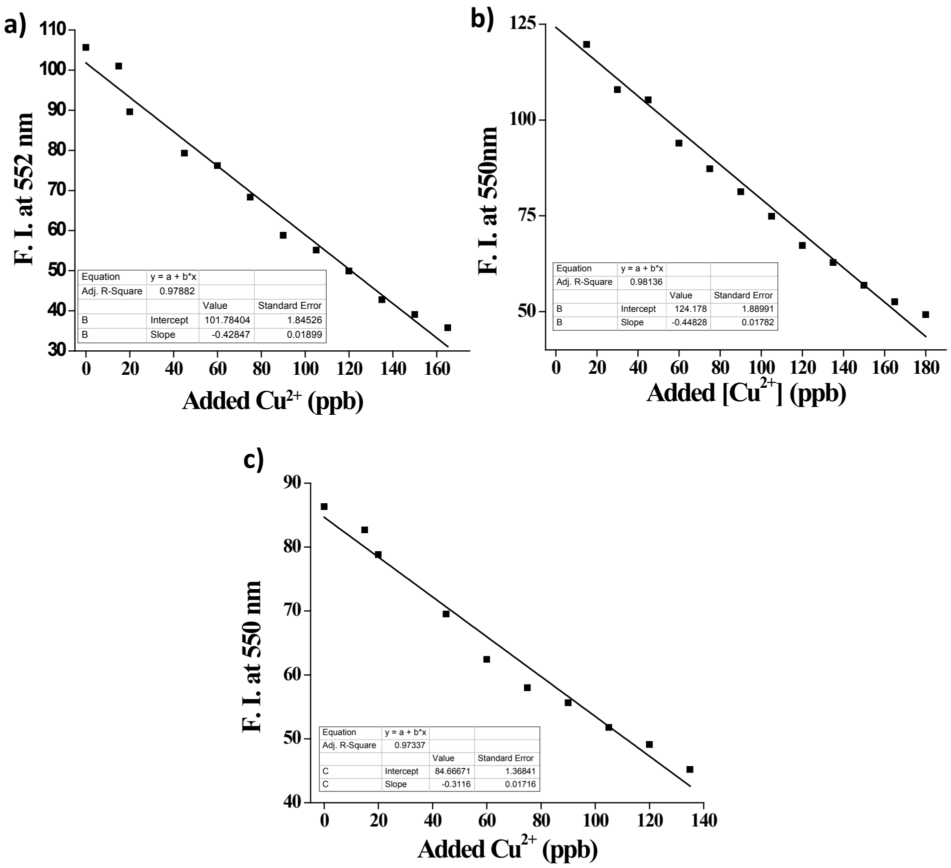

Fig. S18 Changes in the fluorescence intensity of **1** (5 μM) ($\lambda_{ex.}$ = 520 nm) with the added Cu^{2+} in (a) Tap water, (b) Sea water, and (c) swimming pool water.

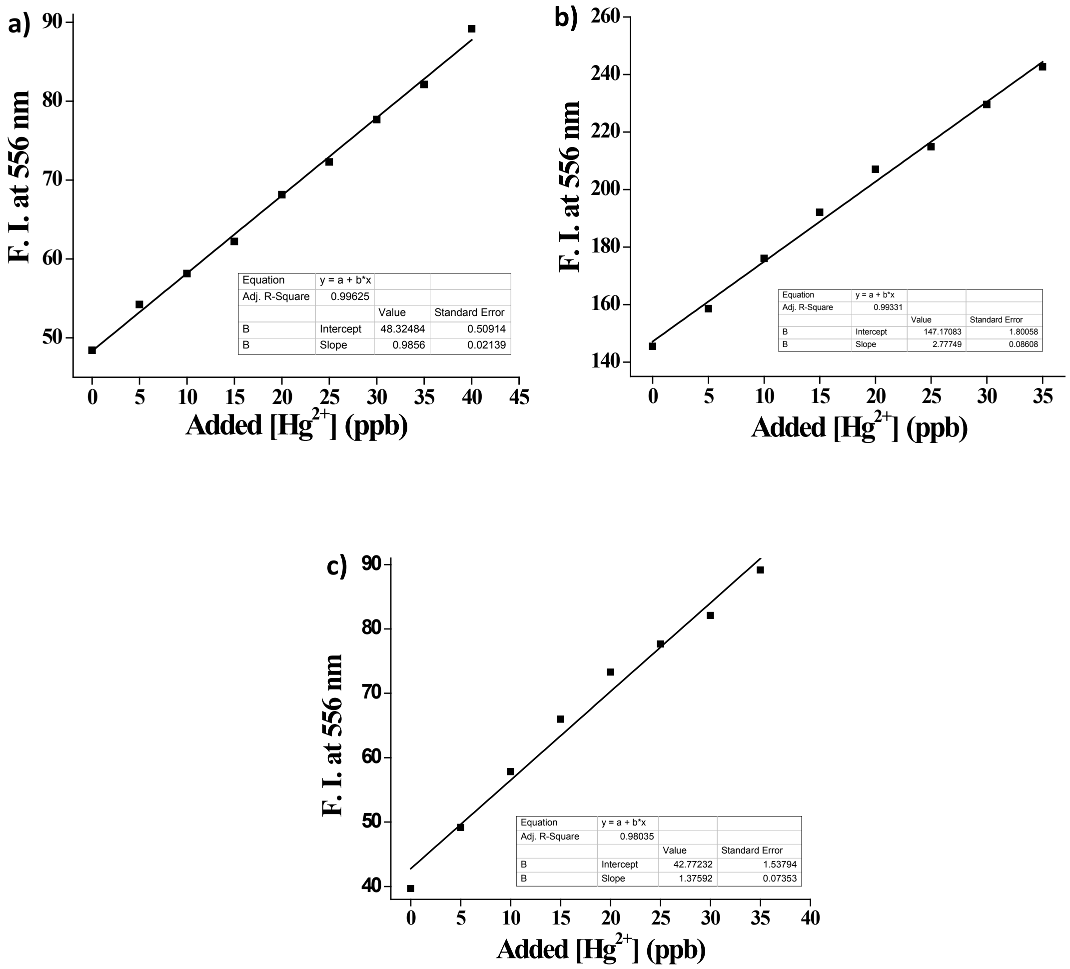

Fig. S19 Changes in the fluorescence intensity of **3** (5 μM) ($\lambda_{ex.}$ = 520 nm) in (a) Tap water, (b) Sea water, and (c) swimming pool water with added Hg^{2+}.

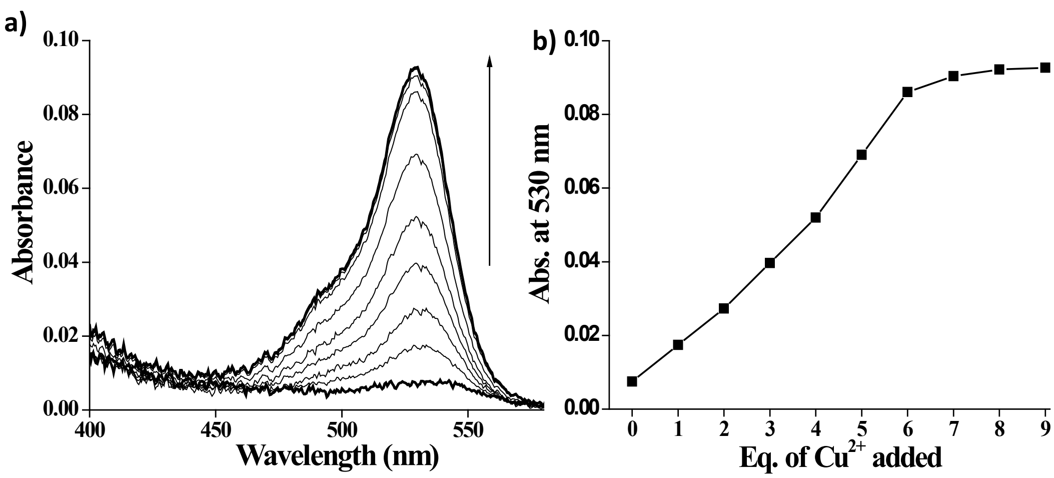

Fig. S20 (a) UV-Vis titration of **1** (10 μM) in BSA (0.1 mg/mL) at pH 7.4 (HEPES buffer, 0.05 M) with Cu^{2+} (0 to 90 μM). (b) Plot of change in the absorbance at 530 nm with the added Cu^{2+} ion.

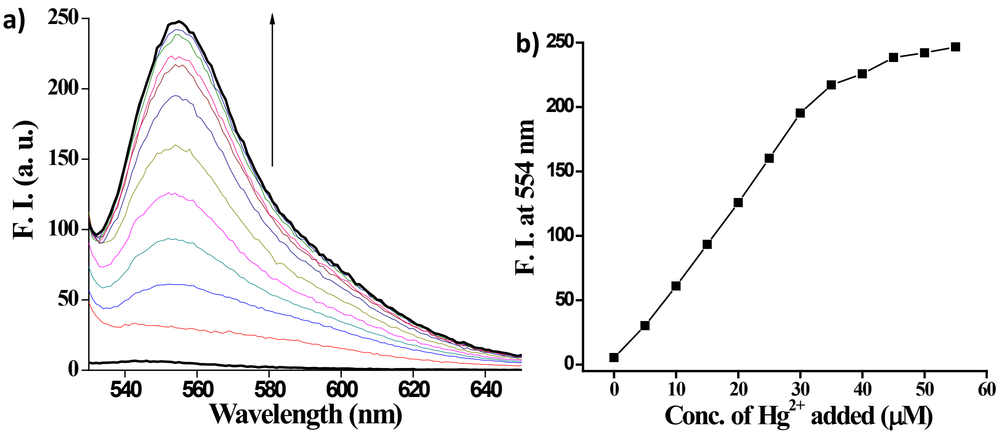

Fig. S21 (a) Fluorescence titration of sensor **3** (5 μM) in water with Hg^{2+} (λ_{ex} = 520 nm) in presence of BSA (0.1 mg/mL). (b) Plot of the emission intensity at 554 nm with the added Hg^{2+} ion.

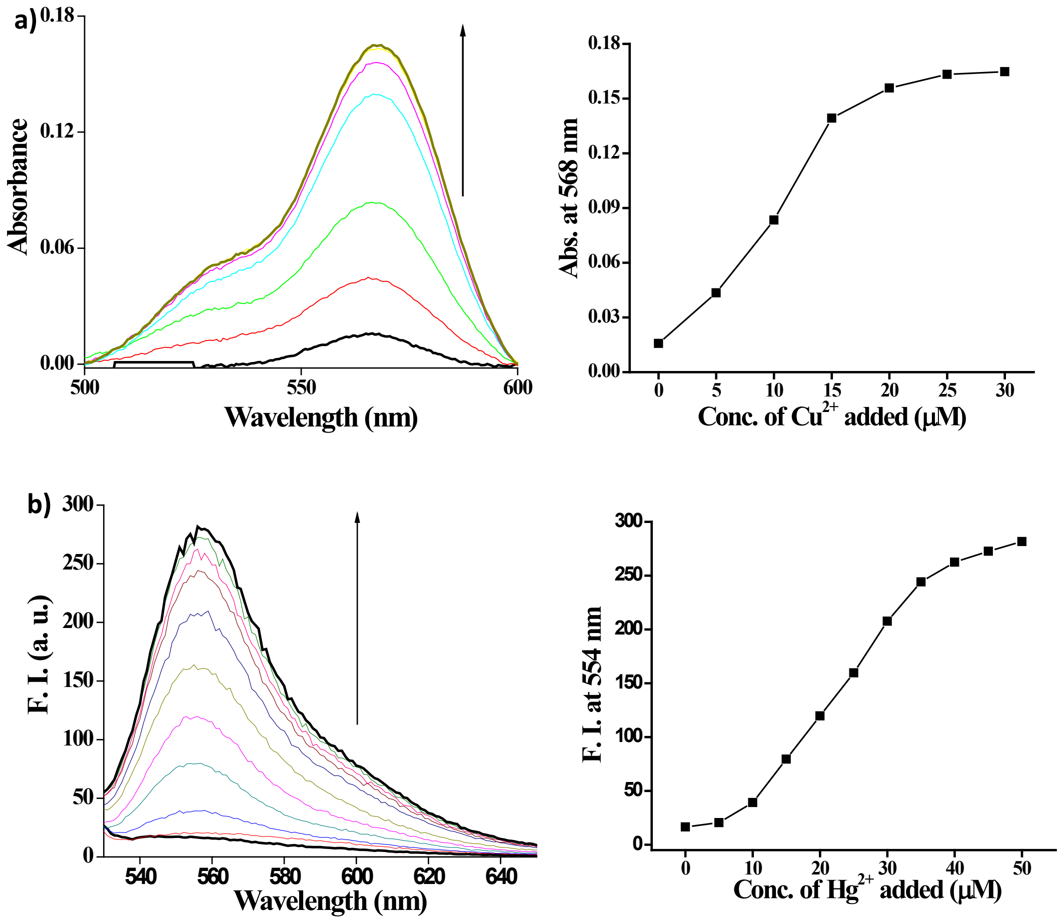

Fig. S22 (a) UV-Vis titration of **1** (10 μM) in blood serum (100 μL) in water with Cu^{2+} (0 to 30 μM) and the corresponding plot of the absorbance at 568 nm with the added Cu^{2+} ion. (b) Fluorescence titration of sensor **3** (5 μM) in water with Hg^{2+} (λ_{ex} = 520 nm) (0 to 50 μM) in presence of blood serum and the corresponding plot of change in the emission intensity at 554 nm with the added Hg^{2+} ion.

.

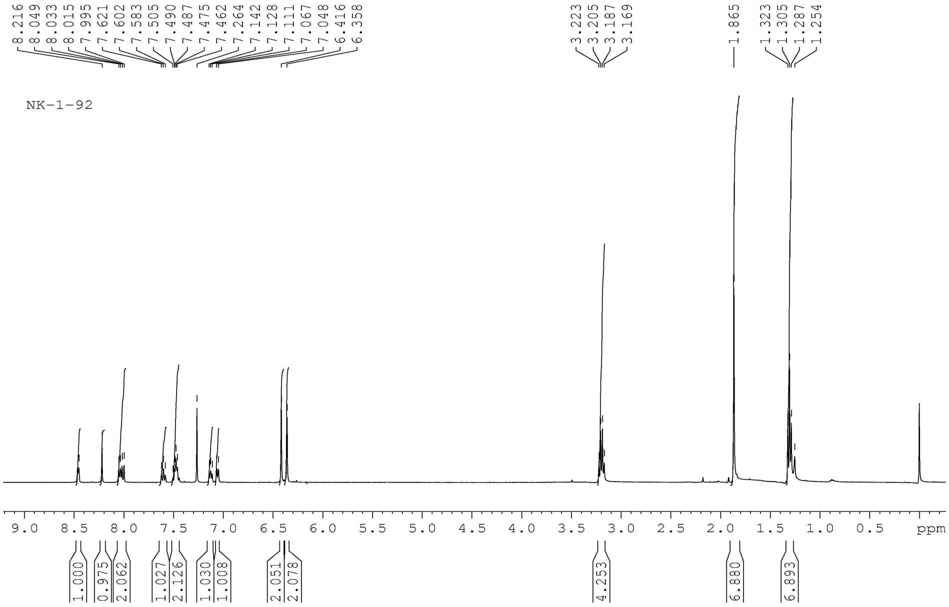

Fig. S23 ^{1}H NMR of compound **1**.

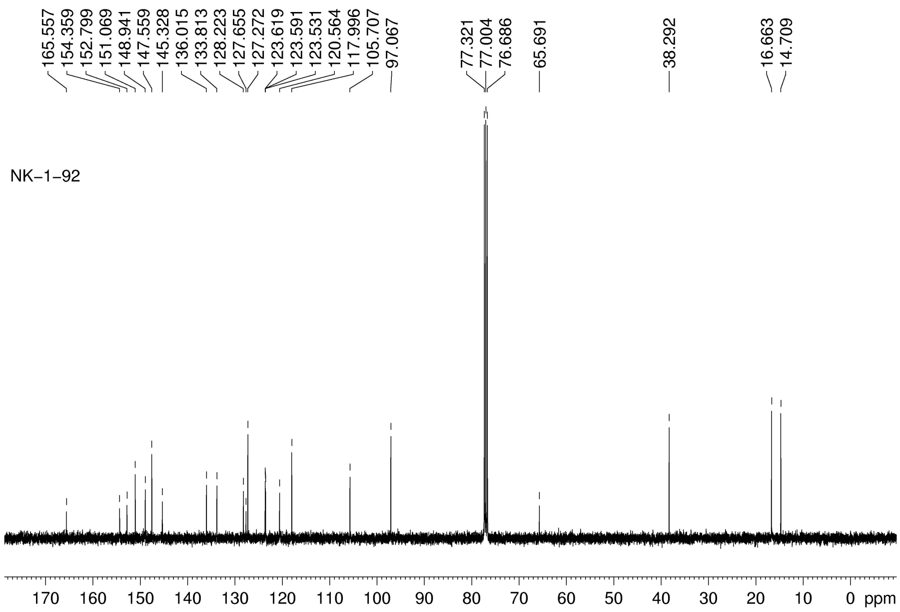

Fig. S24 ^{13}C NMR of compound **1**.

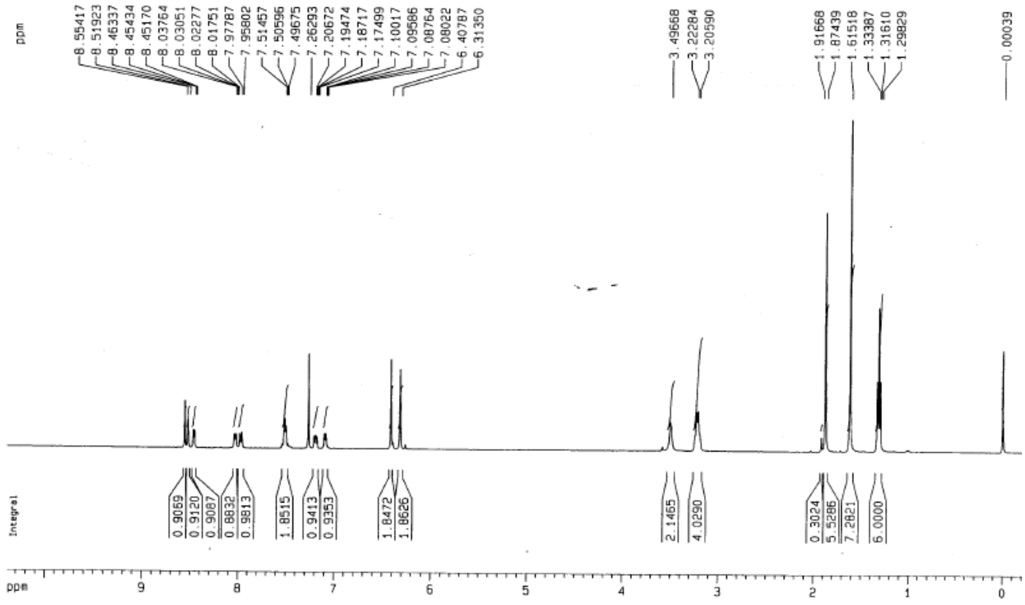

Fig. S25 ^{1}H NMR of compound **2**.

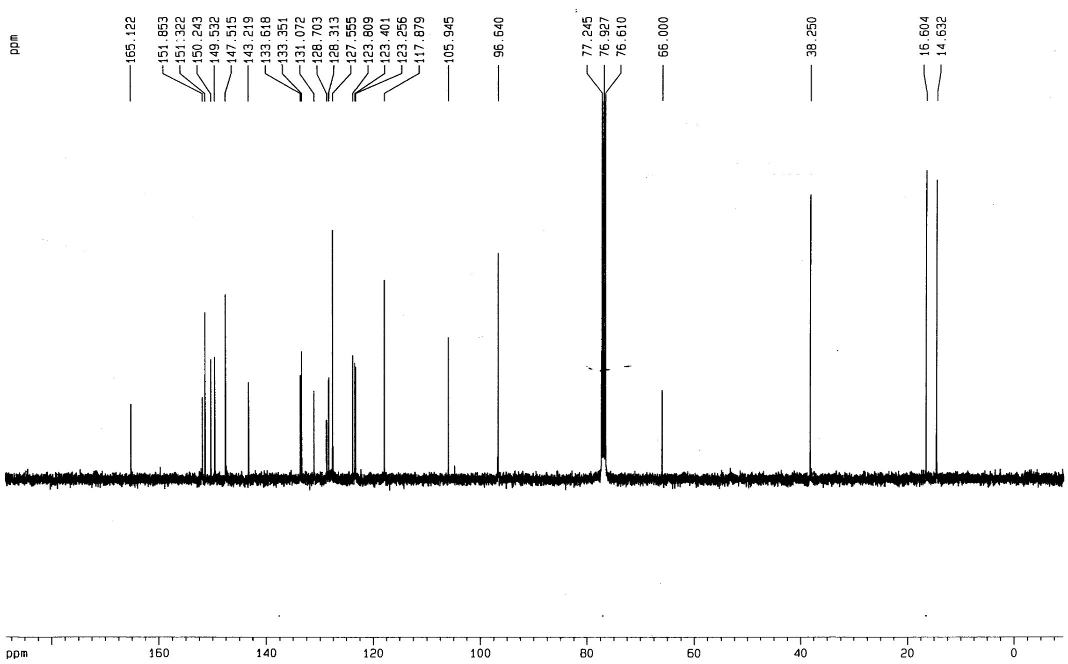

Fig. S26 ^{13}C NMR of compound **2**.

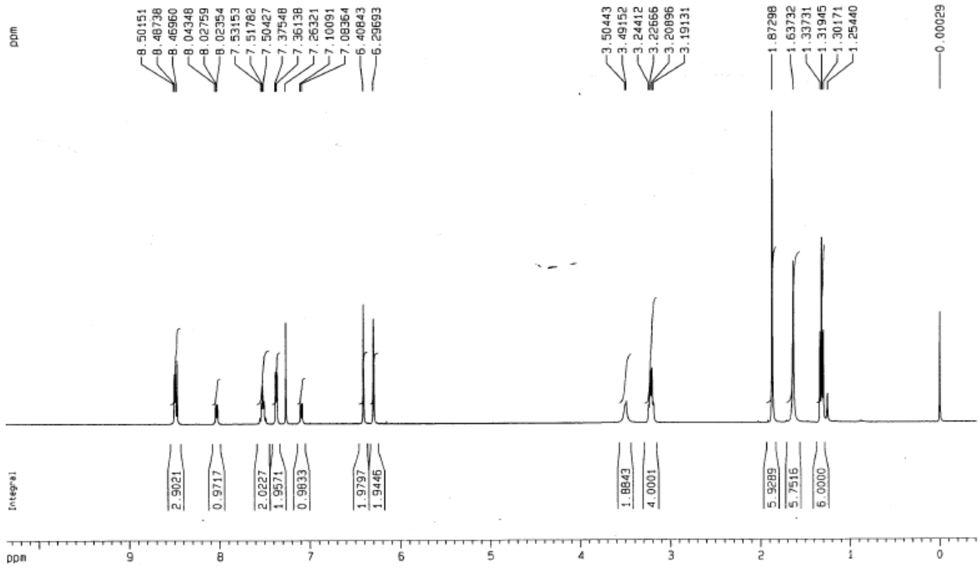

Fig. S27 ^{1}H NMR of compound **3**.

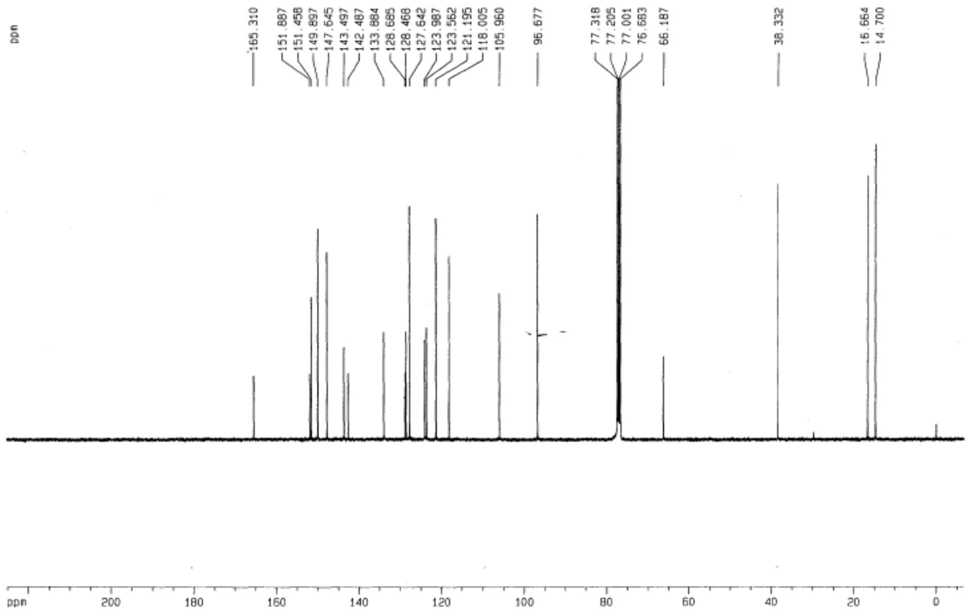

Fig. S28 ^{13}C NMR of compound **3**.

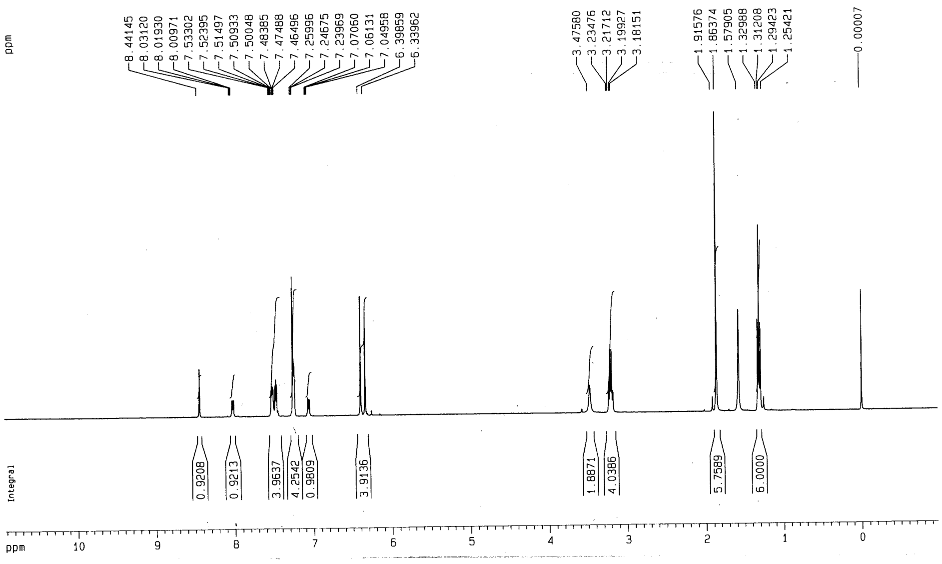

Fig. S29 ^{1}H NMR of compound **4**.

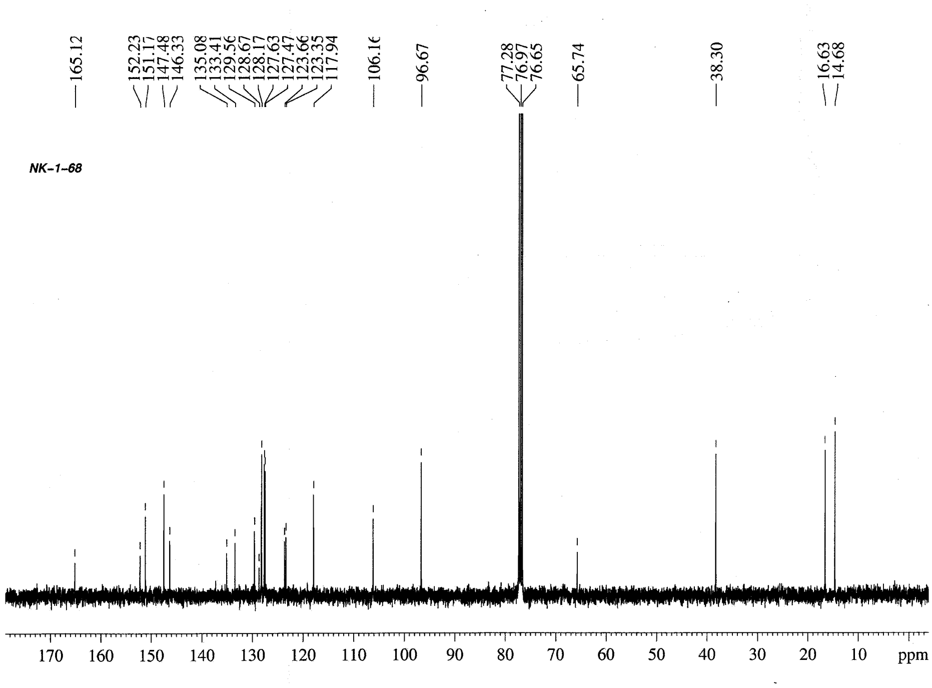

Fig. S30 ^{13}C NMR of compound **4**.